Food Chemistry 463 (2025) 141177

Contents lists available at ScienceDirect

Food Chemistry

journal homepage: www.elsevier.com/locate/foodchem

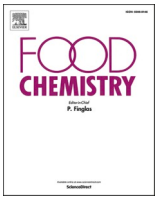

Integration of volatile and non-volatile metabolite profile, and *in vitro* digestion reveals the differences between different preparation methods on physico-chemical and biological properties of *Gastrodia elata*

Shi Li [a], Xiahong He [a,*], Xuechun Zhang [a], Kin Weng Kong [b], Jianhua Xie [c], Jian Sun [d], Zhenxing Wang [a,*]

[a] *Yunnan Provincial Key Laboratory for Conservation and Utilization of In-forest Resource, Key Laboratory for Forest Resources Conservation and Utilization in the Southwest Mountains of China, Ministry of Education, College of Biological Science and Food Engineering, Southwest Forestry University, Kunming 650224, China*
[b] *Department of Molecular Medicine, Faculty of Medicine, Universiti Malaya, Kuala Lumpur 50603, Malaysia*
[c] *State Key Laboratory of Food Science and Technology, Nanchang University, Nanchang 330047, China*
[d] *Guangxi Key Laboratory of Fruits and Vegetables Storage-Processing Technology, Guangxi Academy of Agricultural Sciences, Nanning 530007, China.*

ARTICLE INFO

Keywords:
Gastrodia elata Blume
Processing and drying method
In vitro simulated digestion
Biological activity
Sensory assessment
Metabolite

ABSTRACT

Gastrodia elata Blume (*G. elata*) is a traditional medicinal and edible plant whose quality is significantly influenced by post-harvest processing. To obtain an optimal post-harvest processing method for *G. elata*, this study employed sensory evaluation, scanning electron microscopy (SEM), gas chromatography-ion mobility spectrometry (GC-IMS), and non-targeted metabolomics, in conjunction with an *in vitro* digestion model, to assess the impact of different processing and drying methods on the quality of *G. elata*. The findings showed that the steam treatment followed by heat pump drying resulted in the highest levels of total phenols, total flavonoids, and polysaccharides in *G. elata*, and caused more pronounced damage to its microstructure. This treatment also maintained the highest antioxidant activities and optimal acetylcholinesterase (AChE) inhibition capacity throughout *in vitro* digestion, meanwhile, effectively eliminating the unpleasant odor and achieving the highest sensory scores. Furthermore, non-targeted metabolomic analysis revealed noteworthy alterations in the metabolite profile of *G. elata*, mainly related to purine metabolism and the biosynthesis of amino acids pathways. This study provides valuable insights into the post-harvest processing of *G. elata*.

1. Introduction

Gastrodia elata Blume (*G. elata*), commonly referred to as Tianma in China, is a perennial herbaceous plant belonging to the Orchidaceae genus *Gastrodia* R.Br. It is predominantly distributed across East Asian regions, including China, Japan, Korea, and the Russian Far East, thriving at altitudes between 300 and 2000 m. *G. elata* is extensively utilized in traditional Chinese medicine for its therapeutic effects on the nervous and circulatory systems (Zhan et al., 2016). Furthermore, it possesses a high dietary value and has been consumed in China for over two millennia, leading to its classification by the Chinese government as a medicinal and edible plant (Chinese Pharmacopoeia Commission, 2020).

G. elata is rich in nutrients such as starch, protein, fiber, and minerals. Prior research indicated that *G. elata* contains various active compounds, including phenolics, glycosides, polysaccharides, sterols, organic acids, *etc.* (Li et al., 2019). Furthermore, it demonstrated physiological functions such as reducing blood lipid levels and exhibiting antioxidant, anti-tumor, anti-depression, and anti-inflammatory properties, as well as pharmacological effects like anti-epileptic, anti-convulsant, and memory enhancement (Chen, Liu, Wang, & Qu, 2016; Zeng, Gu, Chen, Zhang, & Zhou, 2021). Therefore, *G. elata* is an excellent medicinal edible plant and has a wide range of potential applications in the fields of food, medicine, health products, and cosmetics.

Abbreviations: G. elata, *Gastrodia elata* Blume; F, Fresh group; SG, Steaming group; CG, Cooking group; WP, Wine processing group; GP, Ginger processing group; HAD, Hot air drying; HPD, Heat pump drying; SD, Sun drying; HPLC, High-performance liquid chromatography; UHPLC, Ultra-high performance liquid chromatography; GC-IMS, Gas chromatography-ion mobility spectrometry; PCA, Principal component analysis; FC, Fold change; VIP, Variable importance in projection; OPLS-DA, Orthogonal partial least squares-discriminant analysis; KEGG, Kyoto encyclopedia of genes and Genomes.

* Corresponding authors.
E-mail addresses: hxh@swfu.edu.cn (X. He), zhenxing_wang@swfu.edu.cn (Z. Wang).

https://doi.org/10.1016/j.foodchem.2024.141177
Received 21 February 2024; Received in revised form 8 July 2024; Accepted 5 September 2024
Available online 7 September 2024

The fresh *G. elata* is prone to quality loss and decomposition, which pose challenges in its storage and processing. Hence, it is essential to employ suitable post-harvest techniques like sun drying, steam drying, oven drying, and roasting to preserve the quality and efficacy of *G. elata*, thus enhancing its storage and usability. Research indicated that various processing methods exerted notably distinct impacts on the quality of *G. elata* (Li et al., 2021; Liu & Huang, 2018). Presently, the research mainly focuses on the influence of specific processing methods, including steaming, boiling, baking, sun drying, fermentation, and drying, on the chemical composition and therapeutic properties of *G. elata*. However, there is limited research comparing the effects of these various processing methods on the flavor, metabolic profile, and biological activity of *G. elata* (Wu et al., 2022). Furthermore, previous studies have solely focused on the changes in the content of active components of the sample during processing, with a noticeable absence of any research on the active ingredients and biological activities of its processed products after absorption and digestion, which are more meaningful for the edible and medicinal value of *G. elata*. Therefore, it is necessary to use various digestion and absorption models to evaluate the digestion, absorption, and metabolic changes of active substances in *G. elata*. Among these, the *in vitro* simulated digestion method is widely used due to its simplicity and cost-effectiveness (Guo et al., 2021).

Based on the content above, to obtain an optimal post-harvest processing method for *G. elata*, this study employed various methods to process and dry *G. elata*. Subsequently, an established *in vitro* simulated digestion model was used to examine the alterations of the active components and biological properties of *G. elata* throughout the digestion process. Then, scanning electron microscopy (SEM), gas chromatography-ion mobility spectrometry (GC-IMS), and ultra-performance liquid chromatography-quadrupole Exactive Orbitrap mass spectrometry (UPLC-Q-Exactive MS) were employed to analyze the microstructures, volatile and non-volatile metabolites of *G. elata* during different processing methods. To our best knowledge, it is the first time the processing method of *G. elata* has been comprehensively investigated, aiming to identify the most suitable processing method for *G. elata*. This study provides data and serves as a theoretical reference for designing an optimal post-harvest process strategy for *G. elata*.

2. Materials and methods

2.1. Materials and reagents

Fresh *G. elata* was purchased in June 2022 from Xiaocaoba Town, Yiliang County, Zhaotong City, Yunnan Province. This region has high altitude (average of 1710 m) and low average annual temperatures (average of 15.5 °C), making it one of the best-producing areas for *G. elata*, with the harvesting season from November onward until June annually. The samples were identified as the tuber of the Orchidaceae plant *Gastrodia elata* Bl. *F. glauca* S. *Chow* by Professor Jianhua Qi from the Botany Teaching and Research Office of the College of Forestry, Southwest Forestry University. In this study, the 2-year-old *G. elata* specimens, measuring 3–5 cm in diameter, 8–12 cm in length, and 200–250 g in weight, and exhibiting a plump, complete, oval shape, uniform size, and an undamaged surface, were chosen for the experiment.

D(+)-anhydrous glucose, Folin-phenol reagent, ferric chloride hexahydrate ($FeCl_3{\cdot}6H_2O$), sodium carbonate (Na_2CO_3), trisodium phosphate (Na_3PO_4), and other chemicals were purchased from Aladdin (Shanghai, China). 2,2′-Azino-bis (3-ethylbenzothiazoline-6-sulfonic acid) (ABTS), 1,1-diphenyl-2-picrylhydrazyl (DPPH), acetylcholinesterase (AChE), acetylthiocholine iodide (ATCI), 5,5′-dithiobis-(2-nitrobenzoic acid) (DTNB), gastrodin, p-hydroxybenzyl alcohol, p-hydroxybenzaldehyde, adenosine, parishin A, parishin B, parishin C and parishin E were all purchased from Meryer Chemical Technology Co., Ltd. (Shanghai, China). α-Amylase, pepsin, trypsin, and bile salt (pig) were purchased from Yuanye Bio-Technology (Shanghai, China). Yellow rice wine (alcohol content is 13 %) was purchased from Kuaijishan Rice Wine Co., Ltd. (Shaoxing, China). Ginger was purchased from local Yonghui Superstores (Yunnan, China).

2.2. Sample preparation

2.2.1. Processing of samples

Fresh *G. elata* with uniform size and consistent quality were washed, peeled, and sliced into pieces 1–1.5 cm thick, achieving a product yield of 91.4 %. Following the guidelines of the Chinese Pharmacopoeia (2020 edition), samples underwent processing using five distinct methods. The first method involved no pre-treatment but only hot air drying at 50 °C for 5 h (referred to as the fresh group, F), resulting in a product yield of 26.3 %. The second method entailed steaming the samples for 10 min (steaming group, SG), followed by hot air drying at 50 °C for 5 h with a product yield of 28.8 %. The third method involved boiling the samples in water at 100 °C for 5 min (cooking group, CG), followed by hot air drying at 50 °C for 5 h with a product yield of 24.7 %. The fourth and fifth methods included adding yellow wine or ginger juice to the fresh *G. elata* slices, allowing them to sit at room temperature for 24 h (referred to as wine processing group, WP, and ginger processing group, GP, respectively), followed by hot air drying at 50 °C for 5 h with product yields of 25.4 % and 26.3 %, respectively.

2.2.2. Drying of samples

Samples were pre-treated as described previously in Section 2.2.1. Based on unified steaming, three drying methods were followed, including hot air drying (HAD) with a product yield of 28.2 %, heat pump drying (HPD) with a product yield of 29.1 %, and sun drying (SD) with a product yield of 24.8 %, respectively. HAD was conducted at 50 °C in an electric hot air drying oven for 5 h, HPD was performed at 50 °C in a heat pump drying equipment (Southeast Wind Technology Co., Ltd., Beijing, China) for 5 h, and SD was done at 23–27 °C under sunlight and ambient air conditions for 24 h, with the environmental average humidity of 50 %.

2.3. In vitro digestion

The method proposed by Xie and colleagues was followed with slight modifications (Xie, Chen, Huang, & Fu, 2020). A 2 g of *G. elata* powder was mixed with 10 mL of distilled water. Subsequently, 10 mL of simulated saliva containing α-amylase (50 U/mg) was added and thoroughly mixed. The pH was adjusted to 6.5, and the mixture was incubated at 37 °C for 15 min. The sample of oral digestion was obtained by collecting the supernatant after centrifugation at 7000*g* for 10 min. The remaining residue was dispersed in 10 mL of distilled water and then mixed with simulated gastric fluid (30,000 U/g pepsin) in equal volume. The pH was adjusted to 2.0, and the mixture was then incubated at 37 °C for 1 h to simulate gastric digestion. The sample of gastric digestion was obtained by collecting the supernatant after centrifugation at 7000*g* for 10 min. The remaining residue was dispersed in 10 mL of distilled water and then mixed with simulated intestinal fluid (250 U/g pancreatin, 30 mg bile salt solution, 54 mg NaCl, and 6.5 mg KCl_2) in equal volume. The pH was adjusted to 7.0, and the mixture was incubated at 37 °C for 2 h. The sample of intestinal digestion was obtained by collecting the supernatant after centrifugation at 7000*g* for 10 min and then filtering it through a 0.22 μm microporous membrane (Digestive fluid information please refer to the Supplementary Table 1).

2.4. Determination of total phenolic content (TPC)

The TPC in the digestion supernatant was analyzed using the Folin-Ciocalteu method with slight modifications (Zhang et al., 2023). Briefly, a mixture comprising 50 μL of the supernatant, 125 μL of 10 % Folin-Ciocalteu solution, and 100 μL of 7.5 % Na_2CO_3 solution was prepared. The mixture was incubated in the dark for 1 h and then the

absorbance at 765 nm was measured. A standard curve was established using gallic acid with concentrations ranging from 0.01 to 0.05 mg/mL. The results were expressed as mg gallic acid/g sample.

2.5. Determination of total flavonoid content (TFC)

The TFC in the digestion supernatant was determined using the sodium nitrite-aluminum nitrate colorimetric method with alterations (Zhang et al., 2023). In brief, 40 μL of the supernatant was mixed with 20 μL of $NaNO_2$ (5 %, *w/v*) and 20 μL of $Al(NO_3)_3$ (10 %, w/v). Following a 6-min reaction, 140 μL of NaOH (5 %, w/v) was added, and the mixture was allowed to react at room temperature for 15 min. The absorbance was subsequently measured at 510 nm. A standard curve was constructed using rutin (0.04–0.2 mg/mL). The results were expressed as mg rutin/g sample.

2.6. Determination of polysaccharide content

The polysaccharide content in different stages of digestion was determined using the phenol-sulfuric acid method with minor adjustments (Zhang et al., 2019). A 50 μL of supernatant was mixed with 50 μL of a 5 % phenol solution, followed by the slow addition of 250 μL of concentrated sulfuric acid. The mixture was then incubated in a water bath at a constant temperature of 40 °C for 10 min. After cooling, the absorbance was measured at 490 nm. A standard curve was generated using D(+)-anhydrous glucose (0.02–0.1 mg/mL). The results were expressed as mg D(+)-anhydrous glucose/g sample.

2.7. Determination of DPPH radical scavenging capacity

The DPPH radical scavenging capacity was evaluated with slight modifications from a previous report (Zhao et al., 2021). Briefly, 100 μL of the supernatant was vigorously mixed with an equal volume of a (0.15 mmol/L) DPPH solution. After incubation in darkness for 30 min, the absorbance was measured at 517 nm. The scavenging rate was calculated using the following formula:

$$\text{Scavenging rate } (\%) = \left(1 - \frac{A_{\text{sample}} - A_{\text{control}}}{A_{\text{blank}}}\right) \quad (1)$$

where A_{sample} = absorbance of the sample group; $A_{control}$ = absorbance of the control group; and A_{blank} = absorbance of the blank group.

2.8. Determination of $ABTS^+$ radical scavenging capacity

The ABTS radical scavenging capacity was determined using a modified version of a previously reported method (Zhao et al., 2021). Briefly, 50 μL of the supernatant was combined with 200 μL of a freshly prepared $ABTS^+$ working solution. After a 6-min reaction at room temperature, the absorbance at 734 nm was measured. The clearance rate was calculated using Eq. (1).

2.9. Determination of acetylcholinesterase inhibition ability

The determination of AChE inhibitory activity was performed with slight modifications to a previously reported method (Sheeja Malar, Beema Shafreen, Karutha Pandian, & Pandima Devi, 2016). Briefly, 50 μL of the sample solution was combined with 125 μL of 3 mmol/L 5,5′-dithiobis-(2-nitrobenzoic acid) and 25 μL of 1 U/mL AChE. After a 15-min reaction at room temperature, 25 μL of 15 mmol/L acetylthiocholine iodide was added, followed by a 10-min reaction at room temperature. The absorbance was measured at 405 nm. The scavenging rate was calculated using the following formula:

$$\text{Inhibition rate } (\%) = \left(1 - \frac{A_{\text{sample}} - A_{\text{blank}}}{A_{\text{control}}}\right) \quad (2)$$

where A_{sample} = absorbance of the sample group; $A_{control}$ = absorbance of the control group; and A_{blank} = absorbance of the blank group.

2.10. HPLC analysis

The HPLC analysis was conducted using an Agilent 1260 LC system (Agilent Technologies, California, USA), and the elution conditions were modified based on a previous report (Wu et al., 2022). The Silgreen C18 chromatographic column (4.6 mm × 250 mm, 5 μm) was employed, with a column temperature set at 35 °C, detection wavelength at 270 nm, injection volume of 10 μL, and flow rate of 1 mL/min. The mobile phase consisted of (A) 0.1 % formic acid water and (B) acetonitrile. The gradient elution conditions were as follows: 0–13 min, 1–1.1 % B; 13–15 min, 1.1–7.2 % B; 15–25 min, 7.2–8 % B; 25–26 min, 8–15 % B; 26–32 min, 15 % B; 32–33 min, 15–37 % B; 33–43 min, 37–40 % B; 43–44 min, 40–100 % B; 44–54 min, 100 % B; 54–55 min, 100–1 % B; and 55–65 min, 1 % B. The filtered sample (10 μL) was measured within the UV scanning range of 200–400 nm. Qualitative and quantitative analyses of the peaks were performed by comparing them with the retention times, peak areas, and standard curves of the reference standards, as shown in Supplementary Table 2.

2.11. Scanning Electron microscope (SEM)

The SEM (GeminiSEM360, Carl Zeiss AG, Germany) was used for micro scanning, with a scanning voltage of 2.00 kV and a magnification of 50 times (Wu et al., 2022). In short, the *G. elata* slices (1 cm × 1 cm × 1 cm) were adhered to the sample stage using conductive adhesive for gold spraying treatment. The gold-sprayed samples were then placed in the scanning electron microscope sample chamber for morphology imaging and analysis.

2.12. Volatile components analysis

The GC-IMS FlavourSpec® flavor analysis instrument (G.A.S. Dortmund, Germany) was utilized for sample analysis. In short, 50 mg of *G. elata* powder was taken into a sealed 20 mL headspace vial. A 1 mL heated syringe was used to automatically extract the headspace of the sample with slight modifications to the previously reported analysis conditions (Feng et al., 2022). The automated injection parameters consisted of an 80 °C incubation temperature, a 15-min incubation time at 500 rpm incubation shaker speed, without split mode, an 85 °C injection needle temperature, and a 100 μL injection volume. The GC conditions were configured with a column temperature of 60 °C and a nitrogen carrier gas (purity ≥99.999 %). The flow rate was programmed as: 0–2 min, 2 mL/min; 2–20 min, 100 mL/min; 20–50 min, 100 mL/min. The IMS conditions were set at a drift tube temperature of 45 °C and nitrogen (≥ 99.999 %) as the drift gas with a flow rate of 150 mL/min. To eliminate cross-contamination, the syringe was purged with nitrogen for 30 s prior to injection and an additional 5 min during each analysis. The obtained results were qualitatively analyzed using the National Institute of Standards and Technology database and the Ion Mobility Spectrum (IMS) database. The volatile components in different processed *G. elata* samples were qualitatively analyzed in two dimensions based on the peak area ratio of an individual volatile compound to the total peak area of all the volatile compounds (% relative content). The system's associated Reporter plugin was used to generate differential spectra between the samples, and the Gallery Plot plugin was used to create fingerprint spectra.

2.13. Sensory assessment

The sensory evaluation standards were developed based on a previous study (Duan et al., 2023), and an evaluation team was established following the guidelines for sensory analysis selection and training (GB/

T14195–93), approved by the Ethics Branch of the Degree Committee of Southwest Forestry University with the approval number SWFU-2023025. Ten subjects (5 males and 5 females, ages 23–25) were informed and consented to participate in the experiment. In this study, *G. elata* slices were placed on a clean plate and evaluated using both olfactory and gustatory senses under natural lighting conditions. The sensory evaluation team consisted of students majoring in food processing and safety from Southwest Forestry University. The sensory descriptors used included the following odors: Fishy, Horse Urine, Pasty, Scorched, and Stink. The taste descriptors included Light Sweet, Astringent, Bitter, Spicy, and Sour. The assessment was conducted using a 9-point preference rating scale, where 1 indicated extremely annoying and 9 represented extremely like, respectively. Please refer to the Supplementary Table 3 for detailed information.

2.14. Untargeted metabolomics analysis

The samples underwent processing using the methods outlined in a previous study in order to facilitate subsequent untargeted metabolomic analysis *via* UPLC-MS/MS. (Gu et al., 2018). A 50 mg of *G. elata* powder was added with 1 mL of methanol-water solution (4:1, *v*/v), and sonicated in an ice bath for 30 min. The mixture was stored at −20 °C for 2 h. Subsequently, the mixture was centrifuged at 16,000*g*, 4 °C for 20 min, and the supernatant was collected for drying in a high-speed vacuum concentrator. A 100 μL of methanol-water solution (1:1, v/v) was then added for reconstitution. Afterwards, the mixture was centrifuged at 20,000*g*, 4 °C for 20 min and the supernatant was collected for mass spectrometry analysis. QC samples were included in the sample queue to monitor and assess the system's stability and the reliability of the experimental data. Chromatographic separation: the samples were analyzed using the Shimadzu-LC30 ultra-high performance liquid chromatography (UHPLC, Waters Milford, MA, USA) system. The chromatographic column used was the Acquity UPLC® HSS T3 (2.1 × 100 mm, 1.8 μm) with a column temperature of 40 °C. The injection volume was 6 μL, the flow rate was 0.3 mL/min, and the mobile phase consisted of a 0.1 % formic acid aqueous solution (A) and acetonitrile (B). The gradient elution conditions were as follows: 0–2 min, 0 % B; 2–6 min, 0–48 % B; 6–10 min, 48–100 % B; 10–12 min, 100 % B; 12–12.1 min, 100–0 % B; 12.1–15 min, 0 % B. The samples were stored in an automated sampler at 4 °C during the entire analysis process. Mass spectrometry acquisition: the samples were detected in both positive ion (+) and negative ion (−) modes using electrospray ionization. The ionization conditions are as follows: spray voltage: 3800v (+) and 3200v (−); capillary temperature: 320 °C (±); sheath gas: 30 (±); aux gas: 5 (±); probe heater temperature: 350 °C (±); S-Lens RF level: 50. The mass scanning range is 70–1050 *m/z*. Data processing: the raw data were processed using MSDIAL software for peak alignment, retention time correction, and peak area extraction. Metabolite structure identification was performed by accurate mass matching (mass deviation <20 ppm) and MS/MS spectral matching (mass deviation <0.02 Da), searching against public databases such as Human Metabolome Database (HMDB), MassBank, and custom-built databases. For the extracted data, ion peaks with missing values >50 % within each group were removed. The positive and negative ion data were normalized by total peak area, integrated, and subjected to pattern recognition using R software. The data were preprocessed using Unit variance scaling for subsequent data analysis.

2.15. Statistical analysis

For statistical analysis, Microsoft Excel, Origin 2018, and IBM SPSS Statistics V.25.0 were used. All experiments were performed in triplicate. The R language package (R 4.0.3) was used for the principal component analysis (PCA) and correlation analysis, and Duncan's test was used to determine significance.

3. Results and discussion

3.1. Selection of processing methods

3.1.1. The content of total phenolic, total flavonoid, and polysaccharide

Fig. 1A (a-l) illustrates the changes in the TPC, TFC, and polysaccharide content of *G. elata* during an *in vitro* simulated digestion process with different processing methods. The letters a-d represent TPC, e-h indicate the TFC, while i-l denotes polysaccharide content. It can be observed that regardless of the preparation method of *G. elata*, the TPC, TFC, and polysaccharide content consistently decrease throughout the digestion process, reaching peak levels during oral digestion and declining during gastric and intestinal digestion stages. Specifically, compared to the undigested samples, the TPC, TFC, and polysaccharide content of *G. elata* after processing decreased by 94.1 %, 95.9 %, and 88.7 %, respectively. For dried *G. elata*, there was a reduction in TPC by 94.0 %, TFC by 95.9 %, and polysaccharide content by 73.9 %. This finding is similar to the results reported by Chen et al. (G. Chen et al., 2015), in their study on the variations of TPC and TFC in 23 different flowers during *in vitro* simulated digestion. Furthermore, Wang et al. (C. Wang et al., 2018) observed a 65 % decrease in the molecular weight of *Inonotus obliquus* polysaccharides following simulated gastrointestinal digestion. The reason is that enzymes or acids in the oral cavity disrupt the bonding between phenolic, flavonoid, or polysaccharide compounds and other substrates, leading to their release (Tarko & Duda-Chodak, 2020). Additionally, during gastric digestion, gastric protease aids the release of these substances, but the acidic environment also triggers oxidation, deglycosylation, hydrolysis, transformation, and cleavage of these compounds, thereby decreasing their levels (Spinola, Llorent-Martinez, & Castilho, 2018). This study indicated that the degradation and transformation of these compounds during gastric digestion exceeded the amount released. In the intestinal digestion phase, a larger number of phenolic, flavonoid, and polysaccharide substances are hydrolyzed by pancreatic proteases and bile or undergo transformation and degradation in an alkaline environment, resulting in a lower release amount than the degradation quantity (Liu et al., 2021). Furthermore, some specific carbohydrate compounds, including glucose, galactose, and fructose, undergo hydrolysis and absorption in the process of intestinal digestion (Tenore, Campiglia, Giannetti, & Novellino, 2015). Overall, *G. elata* polysaccharides are minimally affected by saliva digestion in the oral cavity and require digestion in the stomach and intestines for absorption by the human body.

Comparative analysis revealed that SG, CG, and WP decreased TPC, except for GP. This could be due to the phenolic substances in *G. elata* degraded during the processing and drying, while GP absorbed the phenolic substances from ginger juice. Notably, the SG displayed the highest TPC in both the oral and gastric digestion stages, at 3.88 mg/g and 1.51 mg/g, respectively, and exhibited no significant difference compared to the GP during intestinal digestion. Furthermore, the SG demonstrated significantly higher TPC than the CG and WP in all digestion stages. Regarding TFC, the SG retained the highest value during the undigested and oral digestion stages (4.87 mg/g and 5.11 mg/g), which was significantly higher than that of the other treatment groups. During the gastric and intestinal digestion stages, the TFC in the SG was only notably lower than that in the GP, but not significantly different from the other treatment groups. Additionally, the SG exhibited the highest polysaccharide content at 92.3 mg/g, 68.9 mg/g, and 23.1 mg/g, in each stage of digestion, respectively, which was significantly greater than that of the other groups ($p < 0.05$).

The above results showed that various processing methods have significantly impacted differently on the concentration of active ingredients in *G. elata*. Among them, SG preserved the highest levels of total phenols, total flavonoids, and polysaccharides. Fresh *G. elata* contains various active enzymes, moisture, and respiratory intensity. The SG treatment can effectively destroy or inhibit these active enzymes

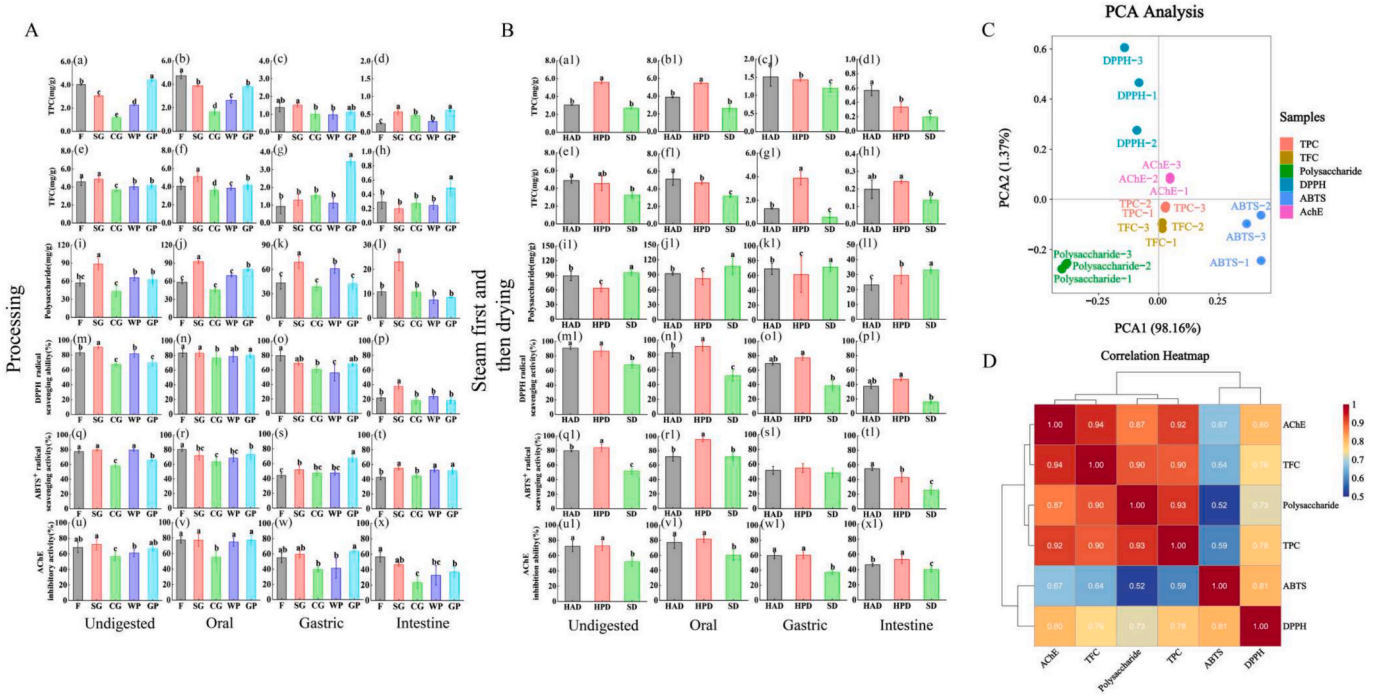

Fig. 1. (A, B) Changes in the TPC, TFC, DPPH radical scavenging capacities, $ABTS^{+}$ radical scavenging capacities, polysaccharide content and AChE inhibitory capacity of *G. elata* at different digestion phase. (a-d, a1-d1) Changes in the TPC; (c-h, c1-h1) Changes in the TFC; (i-l, i1-l1) Changes in the polysaccharide content; (m-p, m1-p1) Changes in DPPH radical scavenging capacity; (q-t, q1-t1) Changes in $ABTS^{+}$ radical scavenging capacities; (u-x, u1-x1) Changes in the AChE inhibitory capacity. At the top of the bar graph, the letters a-c represent the significance analysis of each index during digestion. The labels (a-x, a1-x1) identify each indicator chart. Associations among different indicators. (C) Principal component analysis, (D) Correlation heatmap. The numbers 1–3 represent the three replicates of the sample. F: fresh group; SG: steaming group; CG: cooking group; WP: wine processing group; GP: ginger processing group; HAD: hot air drying; HPD: heat pump drying; SD: sun drying, the same below.

in *G. elata*, leading to a reduction in its respiratory intensity, while also breaking down its cell walls to release its active ingredients (Sharma & Gujral, 2014). Regarding the CG treatment, although it can also inhibit enzyme activity and cause cell wall breakdown, it reduces the active ingredient content and biological activity of *G. elata* through boiling in hot water (Subramaniam, Wen, & Jing, 2020). WP and GP respectively immersed *G. elata* in yellow wine and ginger juice. Although they may diminish the impact of respiratory intensity, both can result in the loss of some active ingredients in *G. elata* (W. Zhang et al., 2021).

3.1.2. Antioxidant capacity

Free radicals are metabolic byproducts produced during various physiological processes in the human body. Excessive free radicals can cause damage to cells, tissues, and organs, accelerate aging, and contribute to the development of diseases. The antioxidant capacity of *G. elata* during the digestive process was evaluated using two methods: the DPPH radical scavenging capacity and the $ABTS^{+}$ radical scavenging capacity. Fig. 1A (m-p, q-t) depicts the trends of *G. elata*'s antioxidant capacity, closely resembling the trends of the active compounds, showing a progressive decrease in antioxidant activity during oral, gastric, and intestinal digestion. This is consistent with the research findings of the *in vitro* simulated digestion process of "*Crataegus pinnatifida*" studied by Zheng et al. (Zheng et al., 2018). A study has demonstrated that substances like phenols and flavonoids can bind to metal ions in the body, thereby inhibiting free radical activity (Rice-Evans, Miller, & Paganga, 1996). Comparatively, the antioxidant capacity of *G. elata* during oral digestion is slightly higher than that of the undigested one. This may be attributed to the release of free phenols during oral digestion, while bound phenols are released after enzymatic action. The progressive stages of digestion resulted in a decreased release of active substances during the gastric and intestinal phases, which correlates with a reduction in antioxidant activity. Fig. 1A (m-t) shows the differences in the antioxidant capacity of *G. elata* with various processing methods. Notably, the SG maintained the highest in antioxidant capacity throughout all stages of digestion, followed by the GP.

3.1.3. AChE inhibitory capacity

AChE catalyzes the hydrolysis and breakdown of acetylcholine, resulting in the depletion of acetylcholine and impaired neuronal transmission. Hence, inhibition of AChE activity is a crucial clinical approach for Alzheimer's disease treatment (Qu et al., 2020). According to Fig. 1A (u-x), *G. elata* exhibited the highest AChE inhibitory activity during oral digestion, followed by gastric and intestinal digestion, these findings corresponded with variations in total phenols, total flavonoids, polysaccharide content, and antioxidant capacity. Similar results have also been reported in previous reports, that gastric and intestinal digestion reduced the sample's AChE inhibitory ability, attributed to the changes in pH levels and the actions of stomach acid, gastric proteases, and pancreatic proteases in the gastric and intestinal stages (Bechaux, Gatellier, Le Page, Drillet, & Sante-Lhoutellier, 2019; Burgos-Edwards, Jimenez-Aspee, Thomas-Valdes, Schmeda-Hirschmann, & Theoduloz, 2017). Overall, *G. elata* maintained relatively high AChE inhibitory activity throughout the entire digestive process. After digestion, *G. elata* maintained AChE inhibitory rates between 23.05 % to 77.37 % across various treatment groups, suggesting its potential as a natural AChE inhibitor. Among them, the SG showed the best inhibitory capacity in almost every digestive stage.

3.2. Selection of drying methods

According to the findings in Section 3.1, the SG exhibited higher levels of active ingredients and demonstrated stronger antioxidant and AChE inhibitory activities. Therefore, steaming is deemed as a more appropriate processing step for *G. elata*. Subsequently, three different

drying methods, including HAD, HPD, and SD were employed to dry the steamed *G. elata*. After drying, the same indicators of each sample after *in vitro* digestion were assessed, such as TPC, TFC, and polysaccharide content, as well as antioxidant activity and AChE inhibitory activity.

From Fig. 1B (a1-d1, e1-h1, i1-l1), under the three drying methods, the changes in TPC, TFC, and polysaccharide content of *G. elata* after digestion were similar by first slightly increasing and then continuing to decrease, which is in line with the results in Section 3.1. Notably, significant differences were observed among the different drying treatments. The trend for TPC and TFC was observed as HPD ≥ HAD > SD, while it was SD > HAD > HPD for polysaccharides. The main reasons for these differences are as follows: the variations in TPC and TFC are primarily influenced by temperature and oxygen concentration, while polysaccharides are mainly affected by the Maillard reaction. The Maillard reaction is influenced by temperature and duration. During HAD and HPD, the samples are exposed to high-temperature air for an extended period, thus hastening the oxidation process, which impacts the levels of TPC and TFC, and also expedites the degradation of sugar substances (Hu, Feng, Huang, Ibrahim, & Liu, 2020). In contrast, SD is conducted at a lower temperature, resulting in a relatively smaller influence on polysaccharides. Nevertheless, at this temperature, the activities of polyphenol oxidase and peroxidase in *G. elata* are relatively vigorous, continuously catalyzing the oxidation of polyphenols and flavonoids, resulting in reduced TPC and TFC (Hu et al., 2020). Overall, the retention capacity of HAD and HPD for these active compounds in *G. elata* is higher than that of SD. This is due to their ability to rapidly reduce the humidity levels in the drying chamber, resulting in higher drying efficiency and reducing the loss of these active compounds.

The digestion of *G. elata* leads to a gradual decline in its antioxidant capacity, displaying a pattern akin to that observed for TPC and TFC. The order of the impact is as follows: oral digestion ≥ undigested > gastric digestion > intestinal digestion (Fig. 1B (m1-p1, q1-t1)). At each stage, the HPD group demonstrated the most superior antioxidant capability. In terms of AChE inhibition activity (Fig. 1B (u1-x1)), the highest activity was observed in the oral digestion stage compared to the undigested samples, with a subsequent progressive decline in the gastric and intestinal digestion stages, which aligns with the changes observed in TPC and TFC. Additionally, HPD also exhibited the most favorable effects at each digestion stage. In conclusion, the optimal approach for preserving the active components and functional activity of *G. elata* is to initially steam it followed by heat pump drying.

To investigate the relationship between the active components and biological activities in *G. elata*, PCA (Fig. 1C) and correlation analysis (Fig. 1D) were conducted. The results from Fig. 1D showed a strong correlation between the antioxidant index and the TPC and TFC, suggesting that TPC and TFC significantly contributed to the antioxidant activity of *G. elata*. The inhibition activity of AChE was influenced by TPC, TFC, and polysaccharides, but PCA confirmed that it is not solely determined by these components. In summary, the functional activity of *G. elata* is the combined result of its various components, rather than being primarily determined by a single type of component. This also demonstrates the characteristic of *G. elata* as having multiple components and targets.

3.3. HPLC analyses

High-performance liquid chromatography (HPLC) was further employed to qualitatively and quantitatively analyze the chemical composition changes in *G. elata* during simulated *in vitro* digestion. The chromatograms at 270 nm of all samples are presented in Fig. 2, and eight standard compounds were distinguished: adenosine (peak 1), gastrodin (peak 2), p-hydroxybenzyl alcohol (HBA, peak 3), parishin E (peak 4), p-hydroxybenzaldehyde (HB, peak 5), parishin B (peak 6), parishin C (peak 7), and parishin A (peak 8).

From Fig. 2, it can be observed that, in each digestion stage, the chromatograms of *G. elata* remain consistent between different processing or drying methods. Still, the chromatographic peak intensities are notably different. It can be observed that the levels of the main effective components such as gastrodin, adenosine, and p-hydroxybenzaldehyde of *G. elata* following SG treatment is relatively higher during the oral, stomach, and intestinal digestion stages, indicating that SG treatment can better preserve the active ingredients in *G. elata*. For different drying treatments, HPD also demonstrated similar optimal results. Regarding the variations of these ingredients throughout the digestion process, irrespective of the processing and drying methods, the chromatographic peaks of *G. elata* also showed a trend of oral digestion stage > gastric digestion stage > intestinal digestion stage. For instance, in Fig. 2C, the HBA content under the SG treatment decreases from 1.243 μg to 0.791 μg, marking a decrease of 36.4 %, further details can be found in Supplementary Table 4 and Table 5. This may be attributed to the degradation or conversion of HBA into other compounds at the gastric digestion stage. Moreover, small chromatographic peaks

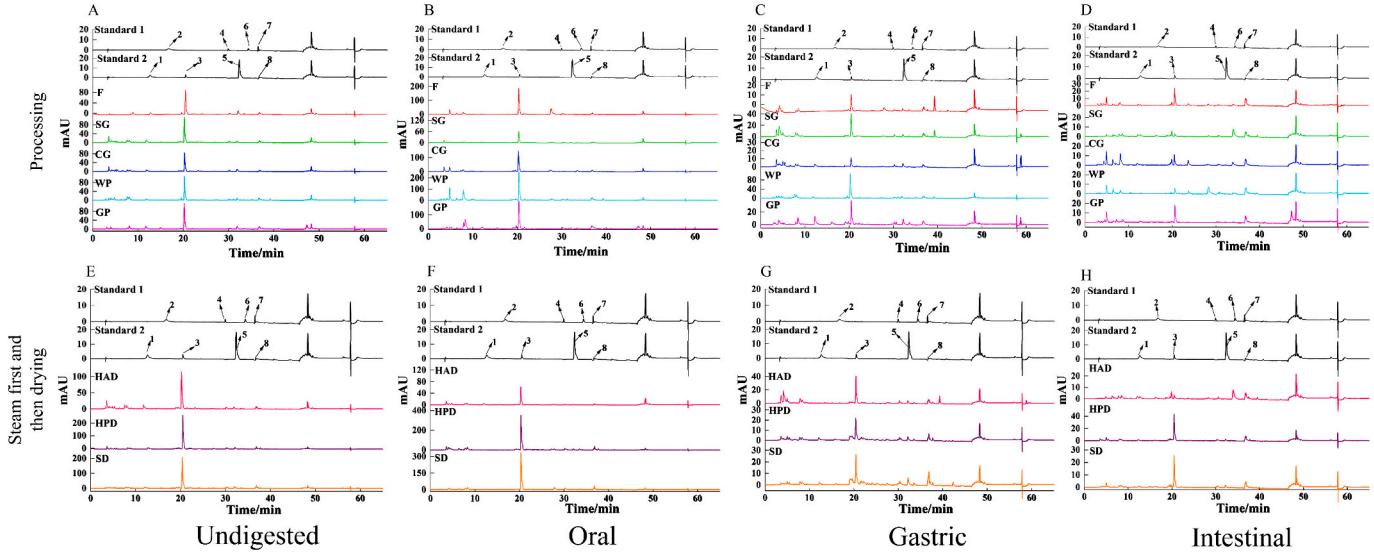

Fig. 2. HPLC chromatogram of the *G. elata*. (A-D) Liquid chromatography diagram of processing of different digestion phase at 270 nm. (*E*-H) Liquid chromatography diagram of steam first and then different drying of different digestion phase at 270 nm. Peak 1: adenosine, Peak 2: gastrodin, Peak 3: p-hydroxybenzyl alcohol (HBA), Peak 4: parishin E, Peak 5: p-hydroxybenzaldehyde (HB), Peak 6: parishin B, Peak 7: parishin C, and Peak 8: parishin A.

gradually emerge in the chromatogram from 20 min onwards, as shown in Fig. 2C and G. In the intestinal digestion phase, the peak intensity of the chromatogram further decreases, with the HBA content reaching 0.051 μg. Similar changes can be observed under different drying treatments, which is consistent with the findings of Jin et al. (Jin et al., 2022) regarding the alterations in phenolic substances during the *in vitro* digestion process of walnuts. Overall, the integration of steaming and heat pump drying is the optimal processing method.

3.4. Scanning electron microscope analyses

Various processing methods induced structural changes in food, consequently impacting the release, stability, solubility, and bioavailability of bioactive compounds (Valadez-Carmona et al., 2017). In this study, the SEM was utilized to visualize the microstructure of *G. elata* after different processing and drying procedures. As depicted in Supplementary Fig. 1 A, the microstructure of untreated fresh *G. elata* (F group) exhibited alternating rings and a tight arrangement. After SG and CG treatments, varying degrees of shrinkage and collapse in the cell wall structure were observed (Supplementary Fig. 1B - 1C), with the SG showing a more pronounced collapse. This can be attributed to the potential pectin degradation within the cell wall caused by high temperatures, subsequently leading to cell wall breakdown and tissue softening. According to previous reports, steaming *G. elata* at temperatures above 55 °C leads to the hydrolysis of polysaccharides, causing the formation of adhesive fragments within the cells (Wu et al., 2022). The treatment of *G. elata* with WP and GP resulted in comparable ruptures and collapses in the microstructure (Supplementary Fig. 1D - 1E). This is attributed to the strong activities of cellulases, ligninases, galacturonases, and pectinases in *G. elata* under these conditions, potentially damaging the structural components of the cell wall.

Similarly, different drying methods lead to discernible variations in both the surface and internal structure of *G. elata* (Supplementary Fig. 1F - 1H). Among them, the external structures of the HAD and HPD groups (Supplementary Fig. 1F - 1G) exhibited more noticeable deformation, collapse, and even rupture, whereas the SD group (Supplementary Fig. 1H) displays minor shrinkage and deformation. In their study, Wu et al. (Wu et al., 2022) investigated the impact of steaming and subsequent drying methods on the microstructure of *G. elata* slices and revealed that phenolic compounds, such as parishin, are frequently bound to the cell wall. Preparatory treatments may promote the release of bioactive compounds by disrupting the cell wall structure.

3.5. Volatile components analysis

By using GC-IMS, a total of 58 volatile compounds were identified in *G. elata,* including 22 aldehydes, 11 hydrocarbons, 7 alcohols, 6 ketones, 3 furans, 3 esters, 1 pyridine, and 5 unidentified substances not found in the database. Further details can be found in Supplementary Table 6 and Table 7.

Overall, the volatile components in *G. elata* predominantly comprise aldehydes, hydrocarbons, alcohols, and ketones. Of which, aldehydes are often formed through lipid oxidation. They possess a distinct aroma at low concentrations due to their low flavor threshold. However, at higher concentrations surpassing the critical value, they can emit a putrid or pungent odor (F. Wang et al., 2021). In *G. elata*, the main aldehydes include nonanal, hexanal, 2-methylbutanal, and 3-methylbutanal. Nonanal contributes to fatty and green fragrances, hexanal adds floral and fruity aromas, while 2-methylbutanal exhibits cocoa and almond notes, and 3-methylbutanal imparts chocolate and peach aromas. Furthermore, various plants, such as tea leaves, chili peppers, and Sichuan pepper, contain a wide distribution of hydrocarbon compounds contributing to their characteristic plant-like and woody aromas (Zhang et al., 2019). *G. elata* primarily contains α-pinene, β-pinene, and limonene as its main hydrocarbons. While α-pinene-D, α-pinene-M, and β-pinene are associated with a pine resin scent, limonene is characterized by a lemon-like odor. The production of alcohols can be triggered by microbial metabolism of proteins and amino acids, alongside lipid peroxidation, leading to the reduction of ketones and aldehydes (Domínguez, Gómez, Fonseca, & Lorenzo, 2014). In *G. elata*, the main alcohols identified are dihydrolinalool, 2-butoxyethanol-D, and 2-butoxyethanol-M. Dihydrolinalool offers a fresh woody fragrance with subtle citrus undertones, while 2-butoxyethanol emits a moderate level of ether odor that can potentially impact flavor negatively. Ketone compounds possess unique flavor characteristics and low flavor thresholds, primarily arising from the β-oxidation of fatty acids and the degradation of amino acids (Licón et al., 2012). Short-chain ketones have fatty and burnt aromas, while long-chain ketones emanate floral scents. The principal ketones identified in *G. elata* include methyl-5-hepten-2-one, 2-heptanone-M, and 2-heptanone-D. Methyl-5-hepten-2-one delivers a fresh and fruity aroma, whereas 2-heptanone-M and 2-heptanone-D exhibit a pear-like fruity scent.

Significant differences in the volatile compounds, particularly aldehydes, hydrocarbons, and ketones, are evident among various processing groups, as demonstrated by the volatile component spectrum (Fig. 3A) and fingerprint spectrum (Fig. 3B). Compared to the untreated group F, significant alterations in specific volatile components were observed in all four treatment groups following processing, and the substances in region a of the fingerprint spectrum demonstrated varying degrees of increase or decrease. As an illustration, the content of (E)-3-penten-2-one increases, whereas 2-n-butylfuran exhibited a decreasing trend. The majority of volatile substances in region b exhibit a substantial increase in content in GP, whereas they remained relatively stable in other groups. Notably, linalool and citronellal remained consistent across all groups. Linalool, known for its lilac fragrance, is associated with potential allergenic properties and has been linked to emotional depression and discouragement (Kamatou & Viljoen, 2008). After processing, the volatile compounds in region c demonstrated a notable increase, primarily concentrated in WP, with a small portion located in GP. These compounds include 3-methylthiopropanal, 2-methylbutanal, and 3-methylbutanal, with 3-methylthiopropanal emanating a strong, pungent odor (Martinez-Arellano, Flores, & Toldra, 2016). It is hypothesized that this compound could be a principal contributor to the distinctive horse urine-like odor emitted by *G. elata.*

Likewise, notable variations in volatile compounds were present among the groups following different drying methods. As illustrated in Fig. 3E, the volatile compounds of HAD, SD, and HPD exhibited similar spectra, with certain compounds demonstrating slight increases or decreases across the different groups. Notably, HPD exhibited a more diverse volatile compound spectrum. In the fingerprint spectra of Fig. 3F, the compounds in the a1 region exhibited a slight overall decrease after heat pump and sun drying treatments compared to HAD. Conversely, the volatile compounds in the b1 region showed minimal change. Aside from a significant increase in volatile compounds in HPD, no other notable changes were observed in the other compounds. For example, furan, 2-methoxy-, and 2-n-butylfuran, which belong to furan compounds, are generated through the thermal decomposition of carbohydrates and contribute to a pleasant baking aroma (Arisseto, Vicente, Ueno, Tfouni, & Toledo, 2011). These changes in volatile components are attributed to variations in temperature, oxygen concentration, enzymatic activity, and other factors during different processing as well as drying procedures, resulting in Maillard reaction, lipid oxidation, degradation, and transformation of precursors, ultimately leading to alterations in the composition and content of volatile components in the raw materials.

The composition and relative contents of volatile compounds in each group of samples are depicted in Fig. 3 (C, G). The findings revealed significant variations in the composition and relative contents of volatile compounds in *G. elata* when subjected to different processing and drying methods. Fig. 3 (D, H) presents the results of PCA analysis, indicating that different processing and drying treatments considerably alter the composition of volatile compounds in *G. elata*.

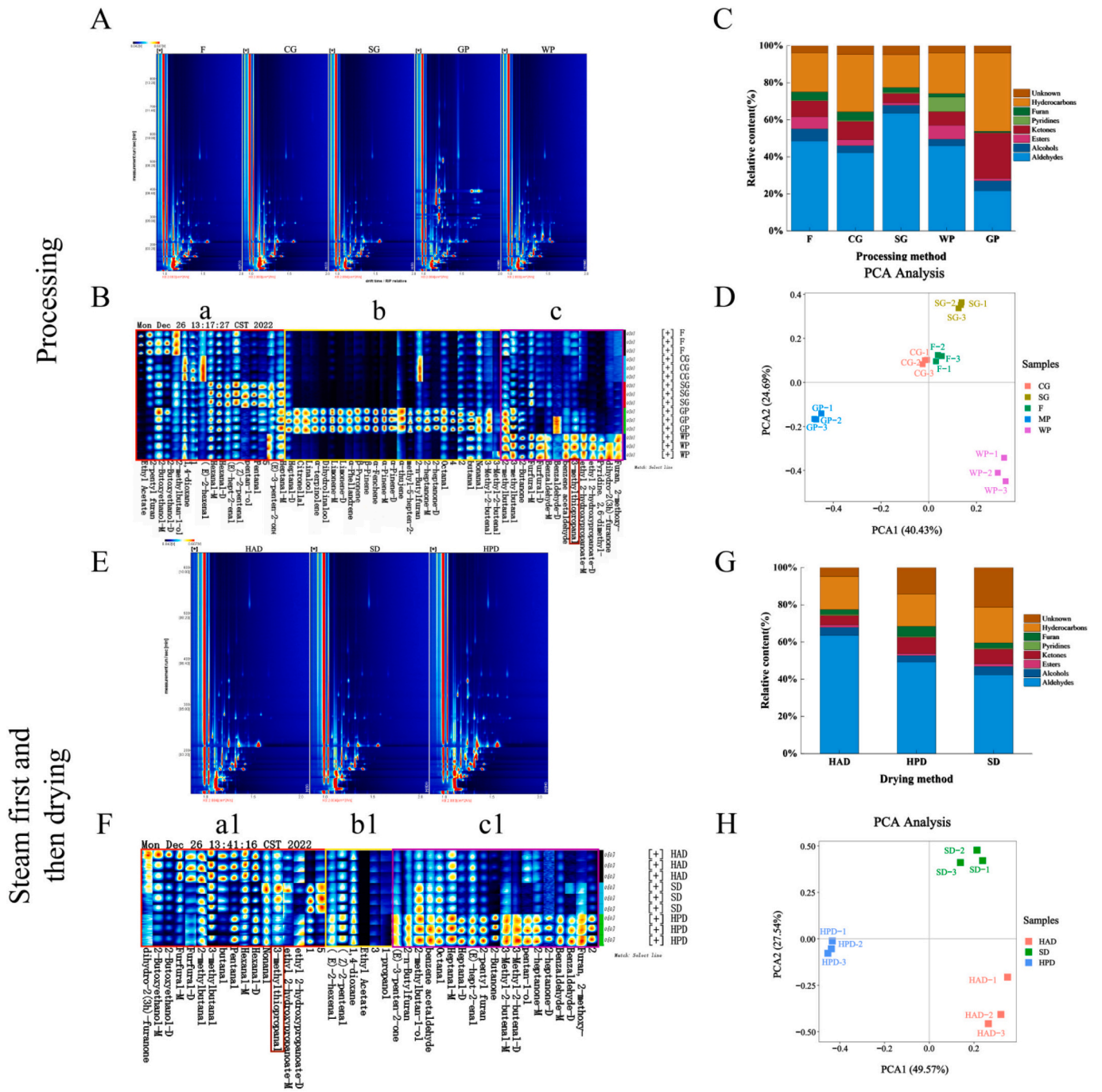

Fig. 3. Analysis of volatile components under different processing methods and steam first and then different drying methods. PCA: principal component analysis, the same below. (A, E) The volatile component spectrum; (B, F) The fingerprint spectrum; (C, G) Differential plot of relative content of volatile compounds; (D, H) Principal component analysis plot.

3.6. Sensory assessment

Sensory evaluation provides an intuitive means of describing and assessing food. A radar chart illustrating the sensory evaluation (Fig. 4A and B) has been plotted by assigning scores to *G. elata* obtained from different preparation and drying methods, revealing significant differences in the sensory evaluation among the different groups. From Fig. 4A, it can be seen that due to the prominent adverse flavors of fishy odor and horse urine odor, the overall score for group F is relatively low. Conversely, the SG demonstrates a significant advantage in sensory evaluations, with the highest ratings in adverse flavors such as fishy odor, pasty taste, bitterness, and spicy taste. This suggests that steaming treatment can effectively alleviate these negative flavors, and also obtain favorable flavors like light sweetness, thereby achieving higher scores. Additionally, steaming treatment significantly improved the horse urine odor ($p < 0.05$), which is considered a key characteristic odor of *G. elata* (Zhan et al., 2016). For the CG treatment, it has been found to effectively reduce negative flavors such as sour taste and astringent taste, especially in alleviating the horse urine odor. As for WP and GP, they significantly enhanced the aroma of scorched odor. Among the three drying methods, HPD showed the most significant effect, followed by HAD and SD (Fig. 4B). It markedly improved the adverse flavors of *G. elata* (sour taste, bitterness, horse urine odor), and increased the palatability of the scorched aroma flavor by 63.4 % compared to

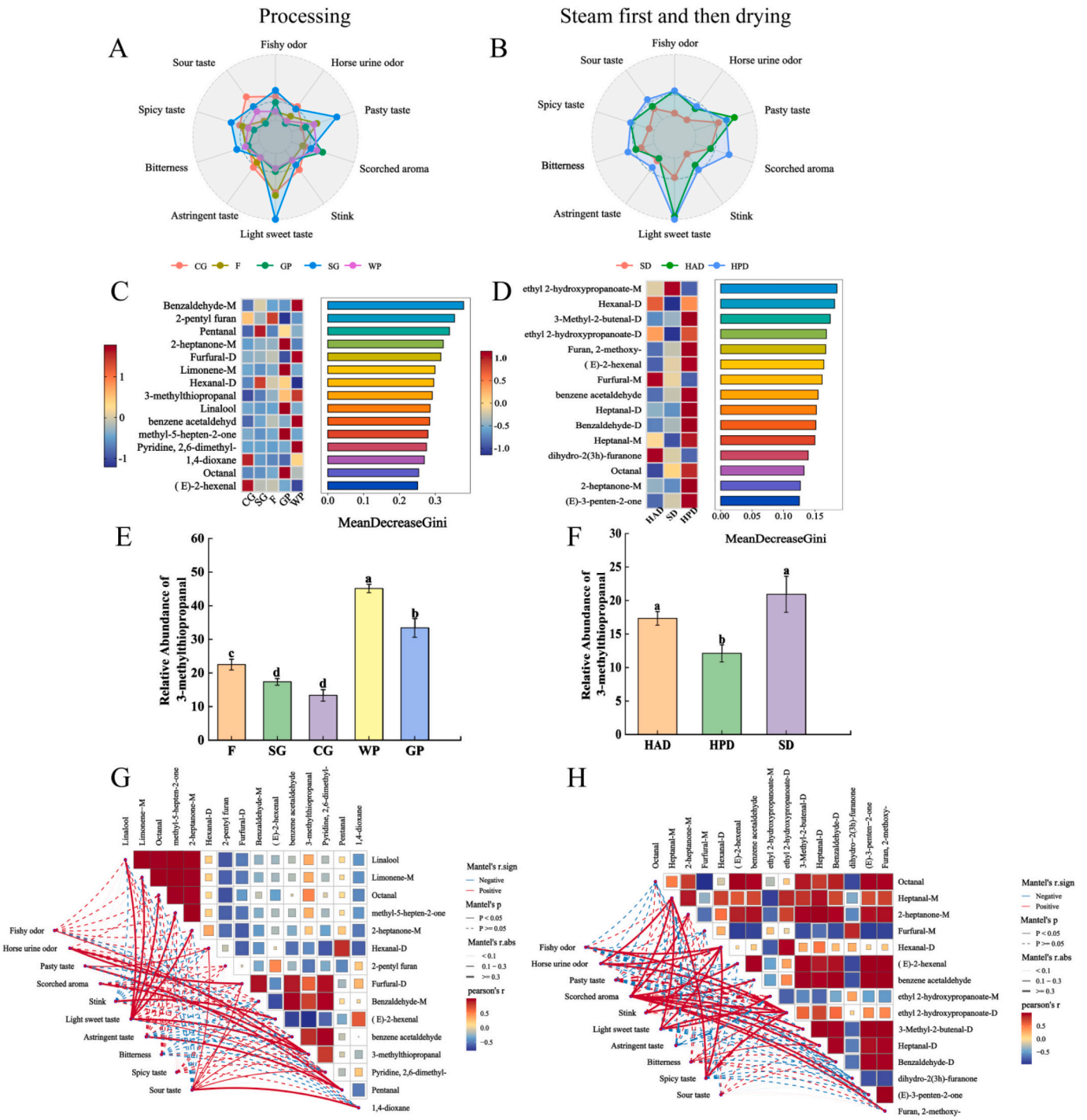

Fig. 4. The radar chart for sensory evaluation of *G. elata*. (A) Radar chart of different processing methods;(B) Radar chart of steam first and then different drying methods.
(C, D) random forest algorithm model; (E, F) The relative content of 3-methylthiopropanal; (G, H) Correlation analysis between sensory evaluation and volatile components with significant differences.

HAD.

Employing a random forest algorithm model to identify the top 15 significantly altered compounds in volatile components in *G. elata* for analysis (Fig. 4C and D), which demonstrated notable alterations in aldehydes, hydrocarbons, and esters following different processing methods. Similarly, comparable results can be achieved after various drying treatments subsequent to steaming. To assess the impact of horse urine odor on *G. elata* after different processing treatments, the relative content of 3-methylthiopropanal (Fig. 4E and F) was compared. The results indicated that SG and CG effectively eliminated the horse urine odor during the processing, while under different drying treatments, HPD also exhibited the capability to remove the odor, indirectly corroborating the sensory evaluation results. To further investigate the influence of volatile compounds on sensory flavor, correlation analysis between the significantly altered volatile compounds (top 15) and the sensory flavor of *G. elata* (Fig. 4G and H) was performed. The figure clearly shows that 3-methylthiopropanal, pyridine,2,6-dimethyi-, pentanal, and 1,4-dioxane significantly influenced the flavor.

3.7. Untargeted metabolomics analysis

To investigate the differences in metabolites resulting from different preparation methods, UPLC-Q-Exactive mass spectrometry was used to carry out the untargeted metabolomics analysis on various processed and dried *G. elata* samples. Initially, the MSDIAL software was used to align the metabolite data, correct retention time, and extract peak areas. Metabolite matching and identification were conducted using accurate mass matching (mass tolerance <20 ppm) and MS/MS spectral matching (mass tolerance <0.02 Da) based on data from HMDB, MassBank, other public databases, and a locally built metabolite standards library provided by Shanghai BIOPROFILE Biotechnology Co., Ltd.

A total of 762 metabolites were identified in *G. elata*, with 507 metabolites detected in positive ion mode and 255 in negative ion mode. Additional details on these metabolites can be found in Supplementary Table 8 and Table 9. The composition and classification of these metabolites were illustrated in Supplementary Fig. 2 through a pie chart. Each color represents a different classification, and the area of each color indicates the relative proportion of metabolites in that classification. From Supplementary Fig. 2, the metabolites in *G. elata* are primarily composed of lipids and lipid-like molecules, organoheterocyclic compounds, and organic acids and derivatives at the SuperClass level. Furthermore, at the Class level, the metabolites consist mainly of steroids and steroid derivatives, prenol lipids, and organooxygen

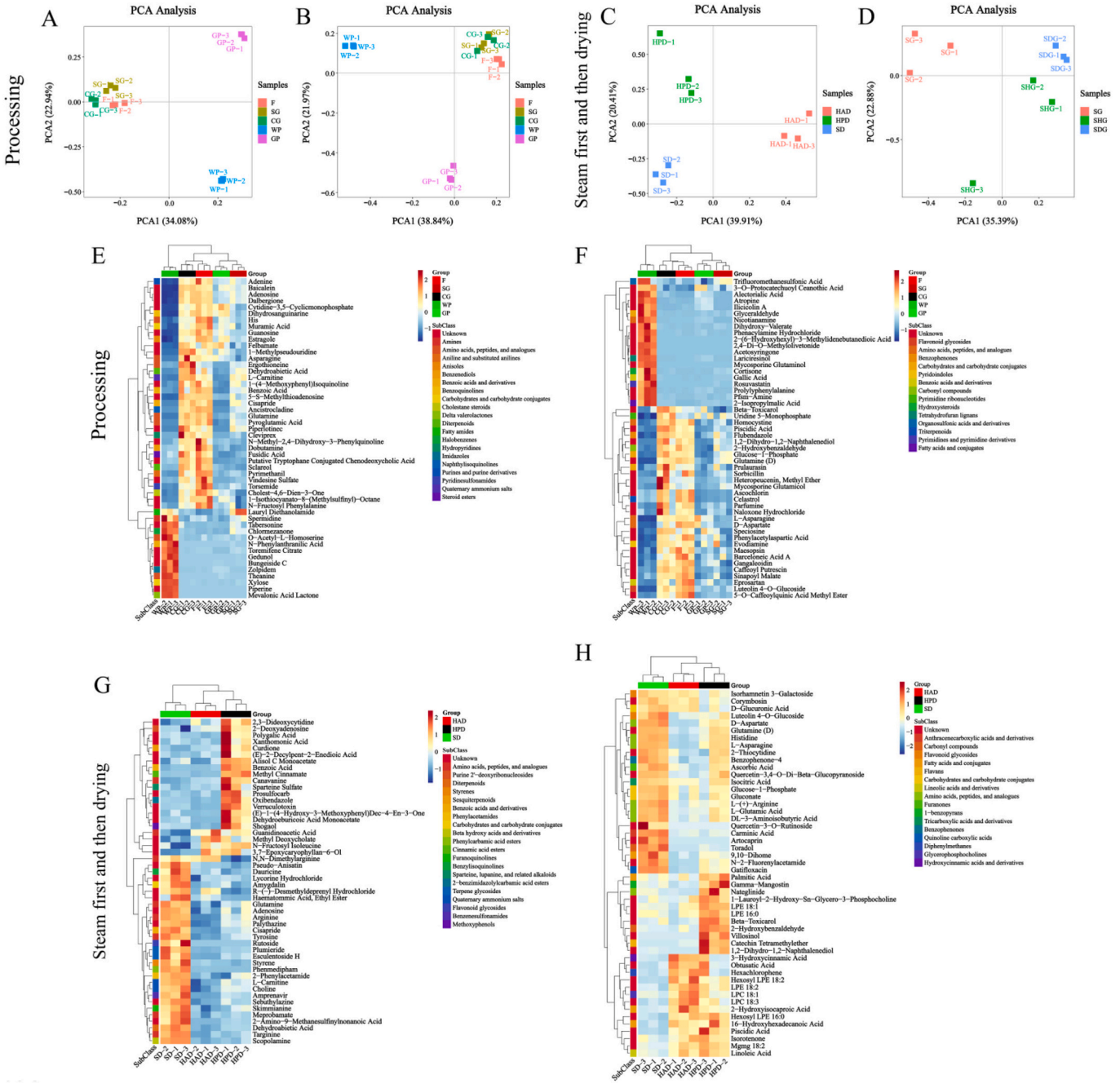

Fig. 5. Analysis of untargeted metabolomics under different processing methods and steam first and then different drying methods. POS: positive ion mode; NEG: negative ion mode. (A, C) Principal component analysis plot in positive ion mode. (B, D) Principal component analysis plot in negative ion mode. (E, G) Heat map in positive ion mode. (F, H) Heat map in negative ion mode. Red denotes relatively high abundance, while blue denotes relatively low abundance. (For interpretation of the references to color in this figure legend, the reader is referred to the web version of this article.)

compounds. Lastly, at the SubClass level, the metabolites primarily include amino acids, peptides, and analogues; carbohydrates and carbohydrate conjugates; as well as benzoic acids and derivatives.

PCA clearly demonstrated the significant differences in the metabolites of *G. elata* among different processing groups (Fig. 5A, B, C, D). The metabolite data underwent analysis using the orthogonal partial least squares-discriminant analysis (OPLS-DA) method to conduct further screening for differentially expressed metabolites between the groups. A total of 228 differential metabolites were identified in the positive ion mode, and 139 in the negative ion mode, (according to VIP value >1 and a p-value < 0.05). Likewise, different drying methods yielded 107 and 53 different metabolites in positive and negative ion modes, respectively.

The top 50 differential metabolites were chosen to construct clustering heatmaps, as shown in Fig. 5E, F, G, and H. The results indicated that the changes in *G. elata* metabolites following different processing treatments focused mainly on amino acids, peptides, and analogues, benzoic acids and derivatives, carbohydrates, and carbohydrate conjugates, as well as diterpenoids. Whereas after undergoing various drying treatments, the alterations primarily involved amino acids, peptides, and analogues, carbohydrates and carbohydrate conjugates, fatty acids and conjugates, flavonoid glycosides, and benzoic acids and derivatives. Comparatively, the metabolites in SG and CG exhibited higher levels of amino acids, peptides, and analogues, whereas WP and GP showed higher levels of metabolites like amino acids, peptides, analogues, and benzoic acids and derivatives. Similarly, HAD, HPD, and SD yielded similar results, with the main distinguishing compounds being amino acids, peptides, and analogues. Among these metabolites,

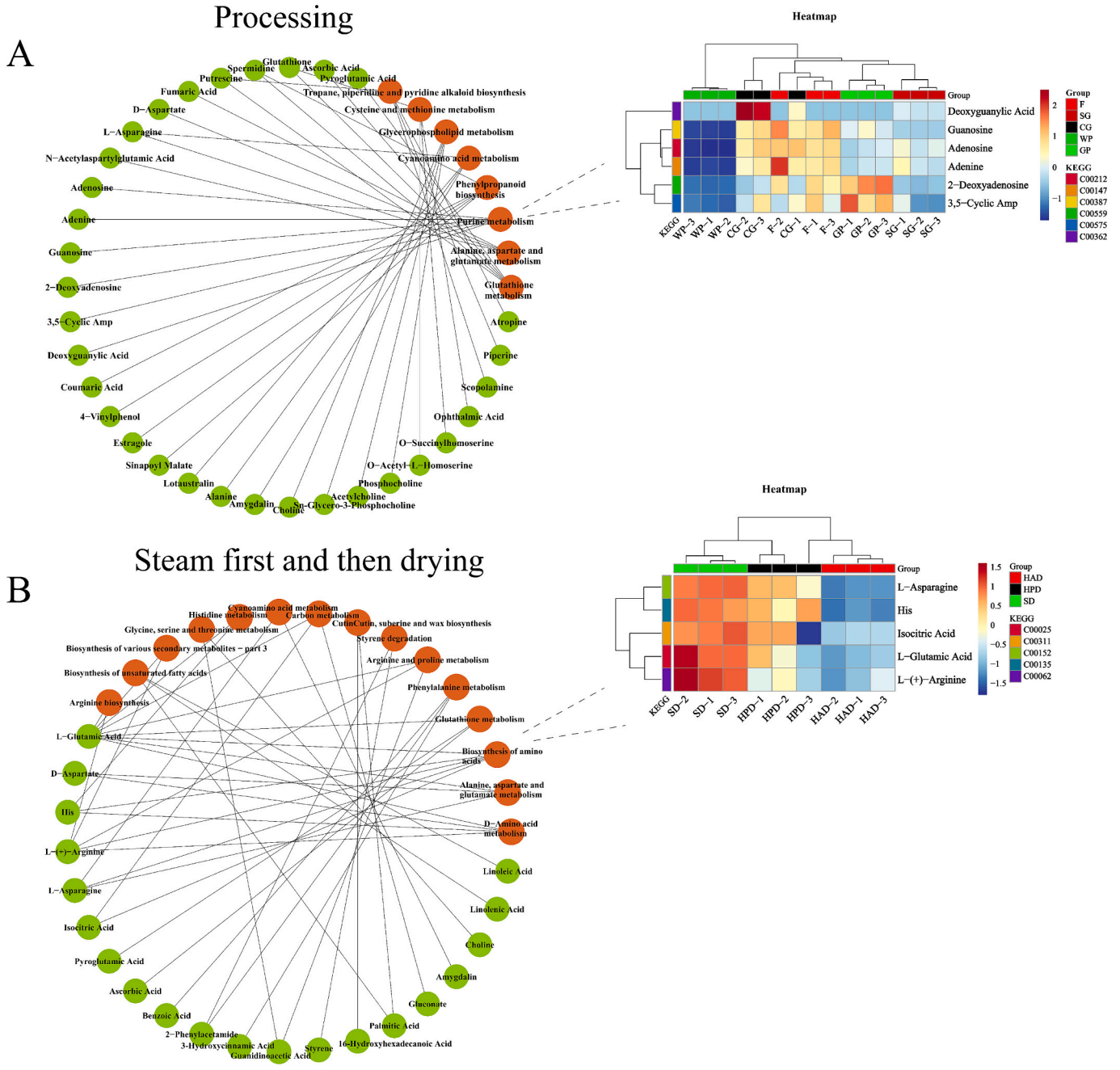

Fig. 6. KEGG pathway network diagram. KEGG: Kyoto encyclopedia of genes and genomes. (A) KEGG pathway of processing; (B) KEGG pathway of steam first and then drying. The orange elliptical nodes represent pathways, and the green elliptical nodes represent metabolites. (For interpretation of the references to color in this figure legend, the reader is referred to the web version of this article.)

luteolin-4-o-glucoside has been reported to possess potent anticancer and anti-inflammatory properties (Xu, Wang, Jiang, Yang, & Wu, 2022), while the vital compound, 3-hydroxycinnamic acid, belonging to the phenylpropanoids and polyketides category, exhibited favorable antioxidant, anti-inflammatory, and antitumor activities in organisms (Taofiq, Gonzalez-Paramas, Barreiro, & Ferreira, 2017). Furthermore, it was found that the hydrolysis of certain proteins generated amino acids that reacted with soluble sugars, enhancing the aroma of *G. elata*. Simultaneously, the breakdown of some flavonoid compounds led to the formation of flavonoid glycosides and sugars, thus reducing the bitterness of *G. elata*. Overall, the changes in these metabolites were the primary cause of the alterations in the functional activities and flavor of *G. elata* post-processing. Spearman correlation analysis (Supplementary Fig. 3 A, 3B, 3C, 3D) further clarified these associations, revealing a significant negative correlation between the capacity to scavenge DPPH radicals and inhibit AChE with the majority of the upregulation metabolites, as well as a positive correlation between the ability to scavenge $ABTS^{+}$ radicals and the majority of the downregulation metabolites. These results specify that the combined action of the various metabolites in *G. elata* determines its functional activities.

In order to investigate the metabolic pathway during the processing and drying of *G. elata*, further Kyoto Encyclopedia of Genes and Genomes (KEGG) pathway analysis was performed on its differential metabolites using data retrieved from the KEGG pathway database (https://www.genome.jp/kegg/pathway.html) on March 23, 2023. A total of 8 and 15 metabolic pathways (Fig. 6A and B) were enriched during the processing and drying stages, respectively. Based on the enriched differential metabolites, it is speculated that the purine metabolism pathway is the primary metabolic pathway of *G. elata* during processing. The purine metabolism in higher plants shares similarities to that found in microorganisms and animals. It encompasses the synthesis, degradation, and utilization of purine nucleotides, as well as the *in vivo* synthesis and decomposition of purine derivatives, such as adenine and guanine (Suzuki, Aahihara, & Waller, 1992). For the drying stage, biosynthesis of amino acids emerged as the most significant metabolic pathway. Amino acids, which are fundamental substances for organisms, can be aerobically metabolized through the tricarboxylic acid cycle to provide energy for the body. In addition to their role in protein synthesis, amino acids also regulate cellular metabolism and biosynthetic pathways, playing a crucial role in organisms (Maeda & Dudareva, 2012). In addition, a heat map was generated to more intuitively demonstrate the variations in key network node metabolite levels between the two most enriched metabolic pathways. Specifically, adenosine, adenine, guanosine, 2-deoxyadenosine, 3,5-cyclic amp, and deoxyguanylic acid were primarily involved in the purine metabolism pathway, while l-glutamic acid, isocitric acid, l-asparagine, his, and l-(+)-arginine were mainly associated with the biosynthesis of amino acids pathway. Overall, many metabolites are engaged in diverse functional activities and contribute to numerous metabolic pathways.

4. Conclusion

In this study, SEM, GC-IMS, UHPLC-MS, and *in vitro* simulated digestion models were used to investigate the effects of different processing and drying methods on the microstructure, volatile components, metabolite profiles, and bioaccessibility of *G. elata*.

The study found that different preparation methods have varying effects on *G. elata*. Overall, the levels of active ingredients and bioactivity of *G. elata* were higher during oral digestion compared to before digestion but decreased as digestion progressed. After processing, there was a significant reduction in TPC, TFC, polysaccharide content, antioxidant capacity, and AChE inhibitory ability of *G. elata*. Similar results were observed for the subsequent drying process. HPLC analysis further revealed the changes in concentrations of eight major compounds in *G. elata* during the digestive process, as well as the differences between different processing methods. Overall, the combined treatment of SG and HPD presented higher levels of active ingredients and stronger functional activity. GC-IMS and GC–MS revealed the differences in the volatile components and flavor of *G. elata* under different processing and drying methods. Specifically, the SG and HPD treatments effectively removed the unpleasant odor of *G. elata*. SEM electron microscopy analysis also revealed greater deformation, collapse, and even rupture in SG and HPD, indicating that these processes enhanced the release of active components in *G. elata*. Untargeted metabolomics analysis showed that both processing and drying resulted in notable and distinct alterations in the metabolite profile of *G. elata*, with purine metabolism and biosynthesis of amino acids identified as the primary metabolic pathways for processing and drying, respectively.

In conclusion, the combination of steaming followed by heat pump drying has been identified as the most effective approach to maintain the active constituents and bioactivity of *G. elata*, making it the method of choice for practical applications. However, this study is constrained by several limitations. Firstly, it investigated only four processing methods and three drying methods. Secondly, the results of *in vitro* simulated digestion experiments may not accurately reflect the complexity of the human digestive system. Lastly, the study only focused on eight active components in *G. elata*, overlooking other potentially significant bioactive compounds. Future research should consider a broader range of processing techniques for comparative analysis and explore in-depth the changes in metabolites during processing, as well as utilize cell and animal models to assess the physiological effects of these metabolites. This research provides a scientific basis for the post-harvest processing of *G. elata*, which is beneficial for its commercial utilization and industrial development.

Ethics statement

The sensory evaluation experiment conducted in this study as a non-clinical human trial has obtained approval from the Ethics Branch of the Degree Committee of Southwest Forestry University under approval number SWFU-2023025. All participants were duly informed of and consented to their participation in the experiment.

CRediT authorship contribution statement

Shi Li: Writing – original draft, Methodology, Investigation, Formal analysis. **Xiahong He:** Writing – review & editing, Project administration, Funding acquisition. **Xuechun Zhang:** Writing – review & editing, Validation, Investigation. **Kin Weng Kong:** Writing – review & editing, Validation, Investigation. **Jianhua Xie:** Writing – review & editing, Validation, Supervision, Investigation. **Jian Sun:** Writing – review & editing, Validation, Investigation, Data curation. **Zhenxing Wang:** Writing – review & editing, Validation, Methodology, Investigation, Conceptualization.

Declaration of competing interest

The authors declare that they have no known competing financial interests or personal relationships that could have appeared to influence the work reported in this paper.

Data availability

Data will be made available on request.

Acknowledgements

This work was supported by the Yunnan Zhengwenjie Expert Workstation (202205AF150018), National Key Research and Development Program of China (2021YFD1000202), Major Science and Technology Project of Yunnan (202102AE090042), Yunnan Province "Support Plan for Prospering Yunnan Talents" Entrepreneurship talents

(2020), and Young Talents (2022,2023).

Appendix A. Supplementary data

Supplementary material: Details of digestive fluid can be found in Supplementary Table 1, The standard curves for the effective components of *G. elata* in HPLC are shown in Supplementary Table 2. Sensory assessment information can be found in Supplementary Table 3. The HPLC analysis revealed the differences in the levels of *G. elata's* effective components resulting from various preparation methods during the *in vitro* simulated digestion process are shown in Supplementary Table 4 and Table 5. The effects of various preparation methods on the volatile components of *G. elata* are shown in Supplementary Table 6 and Table 7. The effects of various preparation methods on the metabolites of *G. elata* are shown in Supplementary Table 8 and Table 9. The effects of various preparation methods on the microstructure of *G. elata* are shown in Supplementary Figure 1. The effects of various preparation methods on the metabolite classification pie chart of *G. elata* are shown in Supplementary Figure 2. The relationship between significant metabolites and functional activity are shown in Supplementary Figure 3.

References

Arisseto, A. P., Vicente, E., Ueno, M. S., Tfouni, S. A., & Toledo, M. C. (2011). Furan levels in coffee as influenced by species, roast degree, and brewing procedures. *Journal of Agricultural and Food Chemistry, 59*(7), 3118–3124. https://doi.org/10.1021/jf104868g

Bechaux, J., Gatellier, P., Le Page, J. F., Drillet, Y., & Sante-Lhoutellier, V. (2019). A comprehensive review of bioactive peptides obtained from animal byproducts and their applications. *Food & Function, 10*(10), 6244–6266. https://doi.org/10.1039/c9fo01546a

Burgos-Edwards, A., Jimenez-Aspee, F., Thomas-Valdes, S., Schmeda-Hirschmann, G., & Theoduloz, C. (2017). Qualitative and quantitative changes in polyphenol composition and bioactivity of *Ribes magellanicum* and *R. punctatum* after *in vitro* gastrointestinal digestion. *Food Chemistry, 237*, 1073–1082. https://doi.org/10.1016/j.foodchem.2017.06.060

Chen, G., Chen, S., Xie, Y., Chen, F., Zhao, Y., Luo, C., & Gao, Y. (2015). Total phenolic, flavonoid and antioxidant activity of 23 edible flowers subjected to *in vitro* digestion. *Journal of Functional Foods, 17*, 243–259. https://doi.org/10.1016/j.jff.2015.05.028

Chen, L., Liu, X., Wang, H., & Qu, M. (2016). Gastrodin attenuates pentylenetetrazole-induced seizures by modulating the mitogen-activated protein kinase-associated inflammatory responses in mice. *Neuroscience Bulletin, 33*(3), 264–272. https://doi.org/10.1007/s12264-016-0084-z

Chinese Pharmacopoeia Commission. (2020). *Pharmacopoeia of the People's Republic of China. Part I*. Beijing: Chinese Medical Science and Technology Press.

Domínguez, R., Gómez, M., Fonseca, S., & Lorenzo, J. M. (2014). Influence of thermal treatment on formation of volatile compounds, cooking loss and lipid oxidation in foal meat. *LWT - Food Science and Technology, 58*(2), 439–445. https://doi.org/10.1016/j.lwt.2014.04.006

Duan, W., Guan, Q., Zhang, H., Wang, F., Lu, R., Li, D., … Xu, Z. (2023). Improving flavor, bioactivity, and changing metabolic profiles of goji juice by selected lactic acid bacteria fermentation. *Food Chemistry, 408*, Article 135155. https://doi.org/10.1016/j.foodchem.2022.135155

Feng, T., Sun, J., Song, S., Wang, H., Yao, L., Sun, M., … Chen, D. (2022). Geographical differentiation of Molixiang table grapes grown in China based on volatile compounds analysis by HS-GC-IMS coupled with PCA and sensory evaluation of the grapes. *Food Chemistry: X, 15*, Article 100423. https://doi.org/10.1016/j.fochx.2022.100423

Gu, Z., Li, L., Tang, S., Liu, C., Fu, X., Shi, Z., & Mao, H. (2018). Metabolomics reveals that crossbred dairy buffaloes are more thermotolerant than Holstein cows under chronic heat stress. *Journal of Agricultural and Food Chemistry, 66*(49), 12889–12897. https://doi.org/10.1021/acs.jafc.8b02862

Guo, Y., Chen, X., Gong, P., Chen, F., Cui, D., & Wang, M. (2021). Advances in the *in vitro* digestion and fermentation of polysaccharides. *International Journal of Food Science & Technology, 56*(10), 4970–4982. https://doi.org/10.1111/ijfs.15308

Hu, S., Feng, X., Huang, W., Ibrahim, S. A., & Liu, Y. (2020). Effects of drying methods on non-volatile taste components of *Stropharia rugoso-annulata mushrooms*. *LWT - Food Science and Technology, 127*, Article 109428. https://doi.org/10.1016/j.lwt.2020.109428

Jin, X., Ru, Y., Zhang, X., Kan, H., Xiang, P., He, X., … Wang, Z. (2022). The influence of *in vitro* gastrointestinal digestion and fecal fermentation on the flowers of *Juglans regia*: Changes in the active compounds and bioactivities. *Frontiers in Nutrition, 9*, 1014085. https://doi.org/10.3389/fnut.2022.1014085

Kamatou, G. P. P., & Viljoen, A. M. (2008). Linalool – A review of a biologically active compound of commercial importance. *Natural Product Communications, 3*, 1183–1192. https://doi.org/10.1177/1934578X0800300

Li, K., Zhang, Y., Wang, Y., El-Kolaly, W., Gao, M., Sun, W., & Li, M. (2021). Effects of drying variables on the characteristic of the hot air drying for *Gastrodia elata*: Experiments and multi-variable model. *Energy, 222*, Article 11982. https://doi.org/10.1016/j.energy.2021.119982

Li, Y., Liu, X., Liu, S., Liu, D., Wang, X., & Wang, Z. (2019). Transformation mechanisms of chemical ingredients in steaming process of *Gastrodia elata* Blume. *Molecules, 24*(17), 3159. https://doi.org/10.3390/molecules24173159

Licón, C. C., Hurtado de Mendoza, J., Maggi, L., Berruga, M. I., Martín Aranda, R. M., & Carmona, M. (2012). Optimization of headspace sorptive extraction for the analysis of volatiles in pressed ewes' milk cheese. *International Dairy Journal, 23*(1), 53–61. https://doi.org/10.1016/j.idairyj.2011.09.003

Liu, X., Shi, J., Yi, J., Zhang, X., Ma, Q., & Cai, S. (2021). The effect of *in vitro* simulated gastrointestinal digestion on phenolic bioaccessibility and bioactivities of Prinsepia utilis Royle fruits. *LWT - Food Scinece and Technology, 138*, Article 110782. https://doi.org/10.1016/j.lwt.2020.110782

Liu, Y., & Huang, G. (2018). The content analysis of Gastrodin and Gastrodigenin obtained by different processing methods. *Journal of Chromatographic Science, 56*(1), 65–67. https://doi.org/10.1093/chromsci/bmx085

Maeda, H., & Dudareva, N. (2012). The shikimate pathway and aromatic amino acid biosynthesis in plants. *Annual Review of Plant Biology, 63*, 73–105. https://doi.org/10.1146/annurev-arplant-042811-105439

Martinez-Arellano, I., Flores, M., & Toldra, F. (2016). The ability of peptide extracts obtained at different dry cured ham ripening stages to bind aroma compounds. *Food Chemistry, 196*, 9–16. https://doi.org/10.1016/j.foodchem.2015.09.023

Qu, Y., Zhan, Q., Du, S., Ding, Y., Fang, B., Du, W., … Huang, W. (2020). Catalysis-based specific detection and inhibition of tyrosinase and their application. *Journal of Pharmaceutical Analysis, 10*(5), 414–425. https://doi.org/10.1016/j.jpha.2020.07.004

Rice-Evans, A. C., Miller, J. N., & Paganga, G. (1996). Structure-antioxidant activity relationships of flavonoids and phenolic acids. *Free Radical Biology & Medicine, 20*, 933–956. https://doi.org/10.1016/0891-5849(95)02227-9

Sharma, P., & Gujral, H. S. (2014). Antioxidant potential of wheat flour chapattis as affected by incorporating barley flour. *LWT - Food Science and Technology, 56*(1), 118–123. https://doi.org/10.1016/j.lwt.2013.10.047

Sheeja Malar, D., Beema Shafreen, R., Karutha Pandian, S., & Pandima Devi, K. (2016). Cholinesterase inhibitory, anti-amyloidogenic and neuroprotective effect of the medicinal plant *Grewia tiliaefolia* – An *in vitro* and *in silico* study. *Pharmaceutical Biology, 55*(1), 381–393. https://doi.org/10.1080/13880209.2016.1241811

Spinola, V., Llorent-Martinez, E. J., & Castilho, P. C. (2018). Antioxidant polyphenols of Madeira sorrel (*Rumex maderensis*): How do they survive to *in vitro* simulated gastrointestinal digestion? *Food Chemistry, 259*, 105–112. https://doi.org/10.1016/j.foodchem.2018.03.112

Subramaniam, S., Wen, X., & Jing, P. (2020). One-step microwave curing-dehydration of *Gastrodia elata* Blume: Relationship between phytochemicals, water states and morphometric characteristics. *Industrial Crops and Products, 153*, Article 112579. https://doi.org/10.1016/j.indcrop.2020.112579

Suzuki, T., Aahihara, H., & Waller, G. R. (1992). Purine and purine alkaloid metabolism in *Camellia* and *Coffea Plants*. *Phytochemistry, 31*, 2575–2584. https://doi.org/10.1016/0031-9422(92)83590-U

Taofiq, O., Gonzalez-Paramas, A. M., Barreiro, M. F., & Ferreira, I. C. (2017). Hydroxycinnamic acids and their derivatives: Cosmeceutical significance, challenges and future perspectives, a review. *Molecules, 22*(2), 281. https://doi.org/10.3390/molecules22020281

Tarko, T., & Duda-Chodak, A. (2020). Influence of food matrix on the bioaccessibility of fruit polyphenolic compounds. *Journal of Agricultural and Food Chemistry, 68*(5), 1315–1325. https://doi.org/10.1021/acs.jafc.9b07680

Tenore, G. C., Campiglia, P., Giannetti, D., & Novellino, E. (2015). Simulated gastrointestinal digestion, intestinal permeation and plasma protein interaction of white, green, and black tea polyphenols. *Food Chemistry, 169*, 320–326. https://doi.org/10.1016/j.foodchem.2014.08.006

Valadez-Carmona, L., Plazola-Jacinto, C. P., Hernández-Ortega, M., Hernández-Navarro, M. D., Villarreal, F., Necoechea-Mondragón, H., … Ceballos-Reyes, G. (2017). Effects of microwaves, hot air and freeze-drying on the phenolic compounds, antioxidant capacity, enzyme activity and microstructure of cacao pod husks (*Theobroma cacao L.*). *Innovative Food Science & Emerging Technologies, 41*, 378–386. https://doi.org/10.1016/j.ifset.2017.04.012

Wang, C., Li, W., Chen, Z., Gao, X., Yuan, G., Pan, Y., & Chen, H. (2018). Effects of simulated gastrointestinal digestion *in vitro* on the chemical properties, antioxidant activity, α-amylase and α-glucosidase inhibitory activity of polysaccharides from *Inonotus obliquus*. *Food Research International, 103*, 280–288. https://doi.org/10.1016/j.foodres.2017.10.058

Wang, F., Yang, X., Xi, B., Wang, H., Li, W., Chen, P., … Gao, Y. (2021). Analysis of fatty acid composition and characteristic flavor fingerprinting of muscles from different anatomical locations of Tan Sheep. *Food Science, 42*, 191–198. https://doi.org/10.7506/spkx1002-6630-20200819-253

Wu, Z., Gao, R., Li, H., Liao, X., Tang, X., Wang, X., & Su, Z. (2022). How steaming and drying processes affect the active compounds and antioxidant types of *Gastrodia elata Bl. f. glauca S. chow*. *Food Research International, 157*, Article 111277. https://doi.org/10.1016/j.foodres.2022.111277

Xie, X., Chen, C., Huang, Q., & Fu, X. (2020). Digestibility, bioactivity and prebiotic potential of phenolics released from whole gold kiwifruit and pomace byin vitrogastrointestinal digestion and colonic fermentation. *Food & Function, 11*(11), 9613–9623. https://doi.org/10.1039/d0fo02399j

Xu, T., Wang, C., Jiang, S., Yang, T., & Wu, X. (2022). Glycosylation of luteolin in hydrophilic organic solvents and structure-antioxidant relationships of luteolin glycosides. *RSC Advances, 12*(28), 18232–18237. https://doi.org/10.1039/d2ra03300c

Zeng, Y., Gu, J., Chen, L., Zhang, T., & Zhou, X. (2021). Gastrodin as a multi-target protective compound reverses learning memory deficits and AD-like pathology in APP/PS1 transgenic mice. *Journal of Functional Foods, 77*, Article 104324. https://doi.org/10.1016/j.jff.2020.104324

Zhan, H., Zhou, H., Sui, Y., Du, X., Wang, W., Dai, L., … Jiang, T. (2016). The rhizome of *Gastrodia elata* Blume – An ethnopharmacological review. *Journal of Ethnopharmacology, 189*, 361–385. https://doi.org/10.1016/j.jep.2016.06.057

Zhang, J., Yang, R., Chen, R., Li, Y., Peng, Y., & Wen, X. (2019). Geographical origin discrimination of pepper (*Capsicum annuum L.*) based on multi-elemental concentrations combined with chemometrics. *Food Science and Biotechnology, 28*(6), 1627–1635. https://doi.org/10.1007/s10068-019-00619-3

Zhang, W., Zheng, S., Wang, Y., Wang, W., Zhang, Z., & Cai, C. (2021). Study on the quality of *Gastrodiae Rhizoma* under different drying and processing methods. *World Science and Technology-Modernization of Traditional Chinese Medicine, 22*(04), 1278–1284. https://doi.org/10.11842/wst.20191121003

Zhang, X., Li, S., Zhang, Z., Kong, K., Wang, Z., & He, X. (2023). Chemical constituents, antioxidant, and α-glucosidase inhibitory activities of different fermented *Gynostemma Pentaphyllum* leaves and untargeted metabolomic measurement of the metabolite variation. *Antioxidants, 12*, 1505. https://doi.org/10.3390/antiox12081505

Zhang, Y., Wang, Y., Yang, S., Xiao, Y., Guan, H., Yue, X., … Li, X. (2019). The difference of chemical components and biological activities of the raw products slices and the wine steam-processed product from *Cistanche deserticola*. *Evidence-based Complementary and Alternative Medicine, 2019*, 1–10. https://doi.org/10.1155/2019/2167947

Zhao, T., Sun, M., Kong, L., Xue, Q., Wang, Y., Wang, Y., … Cheng, G. (2021). Bioactivity-guided isolation of phytochemicals from *Vaccinium Dunalianum* wight and their antioxidant and enzyme inhibitory activities. *Molecules, 26*(7), 2075. https://doi.org/10.3390/molecules26072075

Zheng, G., Deng, J., Wen, L., You, L., Zhao, Z., & Zhou, L. (2018). Release of phenolic compounds and antioxidant capacity of Chinese hawthorn "*Crataegus pinnatifida*" during *in vitro* digestion. *Journal of Functional Foods, 40*, 76–85. https://doi.org/10.1016/j.jff.2017.10.039